Published in IET Networks
Received on 4th July 2012
Revised on 12th November 2012
Accepted on 8th December 2012
doi: 10.1049/iet-net.2012.0136

ISSN 2047-4954

Mitigating shadowing effects through cluster-head cooperation techniques

Petros S. Bithas, Athanasios S. Lioumpas, Angeliki Alexiou

Department of Digital Systems, University of Piraeus, Piraeus, Greece
E-mail: pbithas@unipi.gr

Abstract: In many situations the performance of wireless communication systems decreases especially when they operate over multipath fading channels subject also to shadowing. In this sense, cluster-based networks have been introduced as an efficient solution, offering coverage extension and energy saving. In this study, the authors investigate new cluster-head (CH) selection algorithms, where the nodes can select different CHs, according to the corresponding signal strength. In addition, it is shown that if CHs are equipped with multiple antennas, the negative consequences of fading/shadowing can be further reduced. The performance of this scheme is theoretically investigated over correlated Nakagami-*m* fading channels, which are also subject to shadow fading, modelled by gamma distribution. The derived statistical metrics are used to obtain numerical evaluated results for the outage and the average bit error probabilities. These results are complemented by computer simulated ones, which validate the accuracy of the proposed analysis.

1 Introduction

In recent years, several research activities have been dealing with the assumption of global network infrastructure, proposing novel architectures and technologies towards a dynamic global platform of seamless networks and networked objects [1]. Although a new architecture is required to satisfy the demands of these future systems, it is also essential that their development goes through the enhancement of modern communications networks and standards. In this sense, cellular systems are expected to be a fundamental part of the internet of things, providing them with crucial benefits, such as ubiquitous coverage and global internetworking [2]. However, most of the connected objects (e.g. sensors) are subject to several limitations, including power consumption or hardware complexity, which may hinder direct links to cellular infrastructure. Towards this problem, cluster-based networks have been introduced, providing coverage extension, which facilitates the connectivity of those objects and conserves their energy [3–8].

1.1 Motivation

The envisaged future applications are expected to operate in wireless communication environments, that are subject to low power constraints, fading and shadowing. Although the cluster-based networks offer substantial benefits to such scenarios, the probability of a link failure between the cluster-head (CH) and the nodes cannot be eliminated because of severe channel conditions. In this regard, the energy efficiency, the reliability and the performance of CH networks can be further enhanced if the cluster nodes are able to switch (or select) between different CHs [9–11]. For example, in [10], the authors proposed a protocol to build multiple independent CHs 'overlays' on top of the physical network, which allows the nodes to switch to another CH in case of a CH failure. The CH switch is based on the node's residual energy and a cost parameter that is related with the node's degree of connectivity.

Improving the reliability of wireless links through diversity techniques is an essential concept in wireless communication. Antenna or spatial diversity is an example, highlighting the benefits of combining different replicas of the same information distorted by independent (or near independent) fading paths. Classical diversity reception techniques (at transmit and/or receive sides) include optimal maximal ratio combining (MRC), easily implemented selection diversity (SD) and the least complex switch-and-stay combining (SSC) [12]. In addition, for bridging the performance and implementation gap between MRC and SD, SSC receivers, several hybrid combining techniques have been proposed [12, 13]. Motivated by the fundamental diversity concept, we aim at improving the reliability of cluster-based networks by proposing hybrid link-combining techniques, based on the assumption that the mobile nodes are in the vicinity of two or more CHs [9, 10]. Moreover, prompted by the absence of a theoretical analysis of such hybrid diversity techniques operating over multipath fading channels in the presence of shadowing, we provide a solid mathematical basis for their performance analysis.

1.2 Contribution

To improve the reliability of cluster-based networks through link diversity, and by extending the research framework of

cooperative communication, we investigate two communication protocols, where the nodes can switch between different CHs, according to the corresponding signal strength. More specifically, considering a composite fading environment, where multipath fading coexists with shadowing, and based on the decode-and-forward (DF) strategy, we investigate the case where a message is communicated between a node and an access point (AP), for example, base station or gateway, with the assistance of a number of CHs. In this context,

1. we provide a solid mathematical background for describing the stochastic nature of wireless communication links,
2. we propose two novel communication techniques that determine which CH (in the same CH overlay) is the best option to link the nodes with the AP, according to certain quality of service (QoS) criteria.

The composite fading environment, considered in our case, has been employed several times in the past, for example [14–19]. A common observation in all these works is that independent multipath fading conditions have been assumed, in contrast to our work, where exponential-correlated Nakagami-*m* fading channels, subject also to shadowing, have been considered. Hence, based on the proposed communication techniques, network reliability significantly increases, especially in cases where connection to a CH may not be possible, because of shadowing effects. In contrast to previous works, we relate the CH failure with the quality of wireless link between the infrastructure (e.g. base station), and the node, which is affected by multipath fading and shadowing.

1.3 Outline

The remainder of this paper is organised as follows: in Section 2, the system model along with the basic assumptions is presented. In Section 3, a detailed stochastic analysis provides the theoretical framework of various channel models and case studies. Based on this analysis, in Section 4, different modes of operation are presented, and their corresponding probability density function (PDF), cumulative distribution function (CDF), moments generating function (MGF) and moments of the output signal-to-noise ratio (SNR) are provided. These results are used in Section 5 to study important performance criteria such as bit error probability (BEP) and outage probability (OP). In Section 6, using the above mentioned performance metrics several numerically evaluated results are presented, while in Section 7 the concluding remarks of this paper are provided.

2 System and channel model

We consider a communication network, where a message is communicated between a node and an AP, for example, base station or gateway, with the assistance of a number of CHs [10] (Fig. 1). The APs are considered to support multiple antennas (MAs), whereas CH i, with $i \in (1, N)$, is equipped with a single antenna for the link to the AP and L_i antennas for the link to the mobile nodes. Employing the DF strategy, the CHs decode the signal and then retransmit the detected version to the AP (in case of the uplink), or the destination nodes (in case of the downlink) [20].

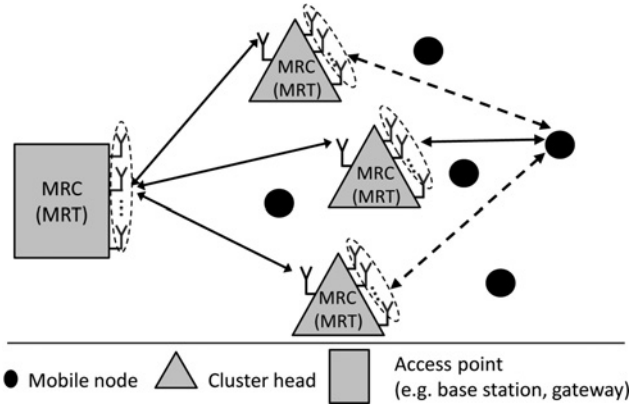

Fig. 1 *System model*

Let $X_{\ell,i}$, with $1 \le \ell \le L_i$, represent the instantaneous SNR per symbol for the link between the ℓth antenna of the ith CH and the mobile node (or the link between the ℓth antenna of the AP and the ith CH). Assuming Nakagami-*m* fading channels, the PDF of $X_{\ell,i}$s is given by

$$f_{X_{\ell,i}}(x) = \frac{m_{\ell,i}^{m_{\ell,i}} x^{m_{\ell,i}-1}}{\bar{x}_{\ell,i}^{m_{\ell,i}} \Gamma(m_{\ell,i})} \exp\left(-\frac{m_{\ell,i} x}{\bar{x}_{\ell,i}}\right), \quad x \ge 0 \tag{1}$$

where $0.5 \le m_{\ell,i} < \infty$ is the distribution's shaping parameter related to fading severity, $\bar{x}_{\ell,i}$ is the average SNR per symbol and $\Gamma(\cdot)$ is the gamma function [21, eq. (8.310/1)]. This model includes the one-sided Gaussian distribution ($m = 1/2$) and the Rayleigh distribution ($m = 1$) as special cases. In the limited case where $m \to \infty$, Nakagami-*m* fading channel converges to a non-fading additive white Gaussian noise channel.

In many practical situations, the radio communication links are considered to be affected by shadowing. In these environments, when the multipath components are also subject to shadowing, $\bar{x}_{\ell,i}$ are randomly varying, becoming thus random variables (RVs). In this environment the receiver does not average out envelope fading because of multipath but rather reacts to the instantaneous composite multipath/shadowed signal [12]. In most cases slow variations in $\bar{x}_{\ell,i}$ are modelled with the lognormal distribution with PDF

$$f_{\bar{x}_{\ell,i}}(y) = \frac{\varsigma}{\sqrt{2\pi}\sigma_{\ell,i} y} \exp\left[-\frac{\left(10\log_{10}(y) - \mu_{\ell,i}\right)^2}{2\sigma_{\ell,i}^2}\right], \quad y \ge 0 \tag{2}$$

where $\varsigma = 10/\ln(10)$ and $\mu_{\ell,i}$ and $\sigma_{\ell,i}$ are the mean and standard deviation of $\ln(\bar{x}_{\ell,i})$. An alternative approach, which has been found to be appropriate for modelling shadowing effects is to employ the gamma distribution [22–24], with PDF given by

$$f_{\bar{x}_{\ell,i}}(y) = \frac{\alpha_{\ell,i}^{\alpha_{\ell,i}}}{\bar{\gamma}_{\ell,i}^{\alpha_{\ell,i}}} \frac{y^{\alpha_{\ell,i}-1}}{\Gamma(\alpha_{\ell,i})} \exp\left(-\frac{\alpha_{\ell,i} y}{\bar{\gamma}_{\ell,i}}\right), \quad y \ge 0. \tag{3}$$

In (3), $\alpha_{\ell,i} \ge 0$ is the shaping parameter of gamma distribution, related to the severity of shadowing (that is smaller values of $\alpha_{\ell,i}$ correspond to stronger shadowing), whereas $\bar{\gamma}_{\ell,i}$ is the average power of $\bar{x}_{\ell,i}$.

The composite fading environment that arises when multipath fading is superimposed on shadowing can be

doi: 10.1049/iet-net.2012.0136

obtained by averaging the PDF of the SNR per symbol, in our case (1) is used, over the conditional density of the average SNR per symbol, statistically described by either the lognormal or the gamma distributions. Mathematically speaking, the total probability theorem can be applied for obtaining the PDF of composite fading SNR as [25, eq. (7.44)]

$$f_{\text{comp-fad}}(\gamma) = \int_0^\infty f_{\text{mult-fad}|\bar{x}_{\ell,i}}(\gamma|y) f_{\bar{x}_{\ell,i}}(y)\,\mathrm{d}y \tag{4}$$

where $f_{\text{mult-fad}|\bar{x}_{\ell,i}}(\gamma|y)$ refers to the PDF that describes multipath fading. It can be easily verified that by using (3), instead of (2), in (4), that is considering gamma distributed shadowing, leads to mathematically more tractable expressions and hence this is the approach that is going to be adopted in our analysis. In the open technical literature and the research framework of cooperative communication over composite fading channels, several works can be found, for example [19, 26–28]. However, to the best of the authors knowledge, none of them investigate the performance of cooperative communication systems that are subject to exponential-correlated fading and shadowing and this is the main scope of this paper.

3 Statistical framework

In this section, based on a useful expression for the sum of Nakagami-*m* RVs, important statistical characteristics of various functions of RVs are investigated. As will be shown later, these expressions are directly related with the network components signals, which are exchanged in the communication system considered in this paper. Let Y_i represent the sum of $X_{\ell,i}$, that is, $Y_i = \sum_{\ell=1}^{L_i} X_{\ell,i}$, and $\rho_{i,j}$ denote exponential correlation among $X_{\ell,i}$s, given as $\rho_{i,j} = \rho_i^{|i-j|}$, $0 < \rho_i < 1$, with $[(i, j) \in (1, \ldots, L_i)]$. Considering also independent and identically distributed (iid) parameters, that is, $\bar{x}_{\ell,i} = \bar{x}_i$ and $m_{\ell,i} = m_i$, the PDF of Y_i is closely approximated by Kotz and Adams [29]

$$f_{Y_i}(\gamma) = \frac{\gamma^{\mathcal{B}_i - 1} \exp\left(-\mathcal{A}_{\bar{x}_i}\gamma\right)}{\Gamma(\mathcal{B}_i)\mathcal{A}_{\bar{x}_i}^{-\mathcal{B}_i}} \tag{5}$$

where

$$\mathcal{A}_{\bar{x}_i} = \frac{m_i L_i}{r_i \bar{x}_i}, \quad \mathcal{B}_i = \frac{m_i L_i^2}{r_i},$$
$$r_i = L_i + \frac{2\rho_i}{1-\rho_i}\left(L_i - \frac{1-\rho_i^{L_i}}{1-\rho_i}\right).$$

Using [21, eq. (3.351/1)] on the definition of the CDF, that is, [25, eq. (4.17)] $\mathcal{F}_{Y_i}(\gamma) = \int_0^\gamma f_{Y_i}(\xi)\,\mathrm{d}\xi$, the corresponding CDF can be obtained as

$$\mathcal{F}_{Y_i}(\gamma) = \frac{\gamma\left(\mathcal{B}_i, \mathcal{A}_{\bar{x}_i}\gamma\right)}{\Gamma(\mathcal{B}_i)} \tag{6}$$

where $\gamma(\cdot, \cdot)$ is the lower incomplete gamma function [21, eq. (8.350/1)].

Moments generating function. Based on the definition of the MGF, that is, [25, eq. (5.62)] $\mathcal{M}_{Y_i}(s) = \int_0^\infty \exp(-s\gamma) f_{Y_i}(\gamma)\,\mathrm{d}\gamma$, and using [21, eq. (3.351/3)], the MGF of Y_i is given by

$$\mathcal{M}_{Y_i}(s) = \left(\frac{\mathcal{A}_{\bar{x}_i}}{\mathcal{A}_{\bar{x}_i} + s}\right)^{\mathcal{B}_i}. \tag{7}$$

Moments. Similar to the derivation of (7) and based on [25, eq. (5.38)], that is, $\mu_{Y_i}(n) = \int_0^\infty \gamma^n f_{Y_i}(\gamma)\,\mathrm{d}\gamma$, the moments can be obtained as

$$\mu_{Y_i}(n) = \frac{(\mathcal{B}_i + n - 1)!}{\Gamma(\mathcal{B}_i)}\mathcal{A}_{\bar{x}_i}^{-n}. \tag{8}$$

3.1 Sum of Nakagami-m RVs averaged on gamma variables

The following statistical metrics are related with combined signals at multiple antennas of the CHs (or the APs) investigated in the next section. Considering also Y_i representing the sum of $X_{\ell,i}$ with PDF provided in (5), whereas $\bar{x}_i$ is an RV following gamma distribution with PDF given in (3). The PDF of Y_i conditioned on $\bar{x}_i$ can be obtained by substituting (5) and (3) in the total probability integral, that is, (4), and using [21, eq. (3.471/9)], yielding

$$f_{Y_i}(\gamma) = \frac{2\mathcal{A}_{\bar{\gamma}_i}^{(\Delta_{i^+})/2}}{\Gamma(\mathcal{B}_i)\Gamma(\alpha_i)}\gamma^{[(\Delta_{i^+})/2]-1} K_{\Delta_{i^-}}\left(2\sqrt{\mathcal{A}_{\bar{\gamma}_i}\gamma}\right) \tag{9}$$

where $\mathcal{A}_{\bar{\gamma}_i} = \alpha_i m_i L_i/(r_i\bar{\gamma}_i)$, $\Delta_{i^+} = \alpha_i + \mathcal{B}_i$, $\Delta_{i^-} = \alpha_i - \mathcal{B}_i$, with identical distributed conditions assumed, that is $\bar{\gamma}_{\ell,i} = \bar{\gamma}_i$ and $K_\nu(\cdot)$ is the modified Bessel function of the second kind and order ν [21, eq. (8.407/1)]. Furthermore, starting from the definition of the CDF [25, eq. (4.17)], expressing $K_\nu(\cdot)$ in terms of the Meijer-*G* function [30, eq. (03.04.26.0006.01)] and using [31, eq. (26)] a closed-form expression for CDF of Y_i can be obtained as follows

$$\mathcal{F}_{Y_i}(\gamma) = \frac{\left(\mathcal{A}_{\bar{\gamma}_i}\gamma\right)^{[(\Delta_{i^+})/2]}}{\Gamma(\mathcal{B}_i)\Gamma(\alpha_i)}\mathcal{G}_{1,3}^{2,1}\left(\mathcal{A}_{\bar{\gamma}_i}\gamma\,\middle|\,\begin{matrix}1 - \frac{\Delta_{i^+}}{2}\\ \frac{\Delta_{i^-}}{2}, -\frac{\Delta_{i^-}}{2}, -\frac{\Delta_{i^+}}{2}\end{matrix}\right) \tag{10}$$

where $\mathcal{G}_{p,q}^{m,n}[\cdot|\cdot]$ is the Meijer's *G*-function [21, eq. (9.301)]. Moreover, using [30, eq. (07.34.03.0727.01)], that is

$$\begin{aligned}
&\mathcal{G}_{1,3}^{2,1}\left(z\,\middle|\,\begin{matrix}a_1\\ b_1, b_2, b_3\end{matrix}\right)\\
&\quad = \pi\csc\left[\pi(b_2 - b_1)\right]\left\{\Gamma(1 - a_1 + b_1)z^{b_1}\right.\\
&\qquad \times \tilde{F}_2(1 - a_1 + b_1; b_1 - b_2 + 1, b_1 - b_3 + 1; z)\\
&\qquad - \Gamma(1 - a_1 + b_2)z^{b_2}\\
&\qquad \left.\times \tilde{F}_2(1 - a_1 + b_2; 1 - b_1 + b_2, b_2 - b_3 + 1; z)\right\}
\end{aligned} \tag{11}$$

where ${}_p\tilde{F}_q(\cdot)$ is the regularised generalised hypergeometric function [30, eq. (07.32.02.0001.01)], a simplified expression for $\mathcal{F}_{Y_i}(\gamma)$ can be extracted.

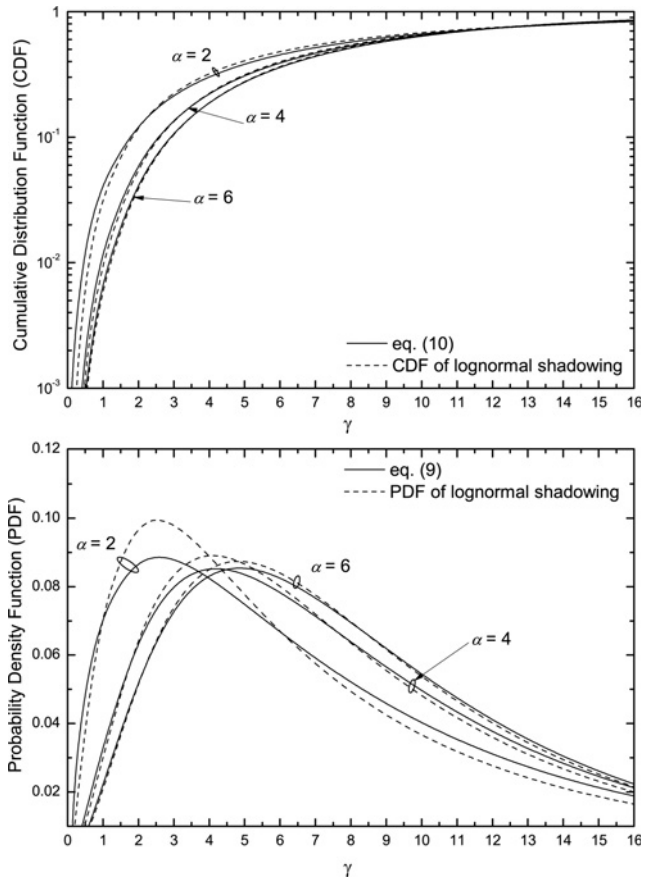

Fig. 2 *Comparison between the proposed PDF and CDF and the corresponding ones obtained when lognormal shadowing is present*

In Fig. 2, considering $m_i = 2$, $L_i = 3$, $\rho_i = 0.5$, $\bar{\gamma}_i = 5$ dB and several values of α_i (it is noted that a one-to-one mapping between α_i and μ_i, σ_i exists in [22]) for $i = 1, 2$, a PDF comparison between (a) (9) and (b) the PDF that is originated by substituting (5) and (2) in (4), evaluated using simulations, is depicted. In the same figure the corresponding CDFs are also illustrated. It can be easily recognised that there is close agreement between these two PDFs, especially for higher values of α_is. Moreover, for further validating the fine agreement between the lognormal and the gamma distributed RVs, we employed the Kolmogorov–Smirnov (KS) goodness-of-fit statistical tests. We compared the analytically evaluated lognormal CDF, with the CDF of the gamma distributed RVs, produced via Monte Carlo simulation. Using 10^5 samples and a significance level of 5%, the KS test was repeated 10^3 times comparing the test statistics with the critical level as calculated in [25]. The average level of acceptance was 97%.

3.1.1 Moments generating function: By substituting (9) in the definition of the MGF [25, eq. (5.62)], and using [21, eq. (6.643/3)], the MGF of Y_i can be expressed as

$$\mathcal{M}_{Y_i}(s) = \mathcal{W}\left(\frac{\mathcal{A}_{\bar{\gamma}_i}}{s}, \alpha_i, \mathcal{B}_i\right) \tag{12}$$

where

$$\mathcal{W}(x, y, z) = x^{[(y+z-1)/2]} \exp\left(\frac{x}{2}\right) W_{[(1-y-z)/2],\,[(y-z)/2]}(x)$$

with $W_{\lambda,\mu}(\cdot)$ denoting the Whittaker function [21, eq. (9.220)].

3.1.2 Moments: The moments of Y_i can be easily obtained by substituting (9) in the definition of the moments [25, eq. (5.38)] as

$$\mu_{Y_i}(n) = \mathcal{R}\left(\mathcal{A}_{\bar{\gamma}_i}, \alpha_i, \mathcal{B}_i\right) \tag{13}$$

where

$$\mathcal{R}(x, y, z) = x^{-n} \frac{\Gamma(y+n)\Gamma(z+n)}{\Gamma(z)\Gamma(y)}$$

3.2 Maximum of two sums of Nakagami-m variables

The following statistical metrics are related with the CH selection process investigated in the next section. Let us define a new RV $Z = \max(Y_1, Y_2)$, with Y_i representing the sum of $X_{\ell,i}$. In that case, and if Y_1 and Y_2 are independent, the CDF of Z can be expressed as [25, eq. (6.55)]

$$\mathcal{F}_Z(\gamma) = \mathcal{F}_{Y_1}(\gamma)\mathcal{F}_{Y_2}(\gamma) \tag{14}$$

while the corresponding PDF can be obtained by differentiating $\mathcal{F}_Z(\gamma)$ with respect to γ as

$$f_Z(\gamma) = f_{Y_1}(\gamma)\mathcal{F}_{Y_2}(\gamma) + \mathcal{F}_{Y_1}(\gamma)f_{Y_2}(\gamma). \tag{15}$$

In the above equation, $\mathcal{F}_{Y_i}(\gamma)$ is given by (10), whereas $f_{Y_i}(\gamma)$ is given by (9).

3.2.1 Moments generating function: By substituting (9) and (10) in (15) and using the definition of the MGF, a closed-form expression for MGF of Z cannot be obtained. To overcome this, the Meijer-G function appearing in (10) is expressed in terms of ${}_p\tilde{F}_q(\cdot)$, with the aid of (11), and then by employing the infinite series representation of ${}_p\tilde{F}_q(\cdot)$, [30, eq. (07.32.02.0001.01)], integrals of the following form appear

$$\mathcal{I} = \int_0^\infty x^{c_1} \exp(-C_1 x) K_{c_2}\left(C_2 x^{1/2}\right) \mathrm{d}x \tag{16}$$

where $c_1, c_2, C_1, C_2 \in \mathbb{R}$ with $c_1 > |c_2/2|$. These integrals can be solved in closed form, using [21, eq. (6.631/3)], and hence after some mathematical manipulations, the following exact expression for MGF of Z can be extracted

$$\mathcal{M}_Z(s) = \sum_{j=1}^{2} \frac{\mathcal{D}_j \mathcal{D}_\xi \pi \csc(-\pi\Delta_{\xi^-})}{s^{\left[\left(\Delta_{j^+}-1\right)/2\right]}\sqrt{\mathcal{A}_{\bar{\gamma}_j}}} \exp\left(\frac{\mathcal{A}_{\bar{\gamma}_j}}{2s}\right) \times \left[\mathcal{H}_1\left(\alpha_\xi, \alpha_j, \mathcal{A}_{\bar{\gamma}_j}, \mathcal{B}_j, \mathcal{A}_{\bar{\gamma}_\xi}, \mathcal{B}_\xi, s\right) - \mathcal{H}_1\left(\mathcal{B}_\xi, \alpha_j, \mathcal{A}_{\bar{\gamma}_j}, \mathcal{B}_j, \mathcal{A}_{\bar{\gamma}_\xi}, \alpha_\xi, s\right)\right] \tag{17}$$

doi: 10.1049/iet-net.2012.0136

where

$$\mathcal{H}_1(x, y, z, q, w, r, s) = \sum_{t=0}^{\infty} \frac{\Gamma(x+t+y)}{\Gamma(x-r+1)x} \frac{(x)_t w^{\{t+[(x-r)/2]\}} \Gamma(x+t+q)}{(x-t+1)_t (x+1)_t s^{x+t} t!} \times W_{[(1-y-q)/2]-x-t,\,[(y-q)/2]}\left(\frac{yz}{s}\right)$$

while $\mathcal{D}_i = \left(\mathcal{A}_{\overline{\gamma}_i}^{[(\Delta_{i^+})/2]}\right)/\left(\Gamma(\mathcal{B}_i)\Gamma(\alpha_i)\right)$, $(\cdot)_p$ is Pochhammer's symbol [21, p. xliii], with $p \in \mathbb{N}$, and $\xi = 3 - j$. In Section 6, the convergence rate of the series appearing in (17) is also examined, verifying its fast convergence.

3.2.2 Moments: Substituting (9) in the definition of the moments, expressing $K_\nu(\cdot)$ in terms of the Meijer-G function [30, eq. (03.04.26.0006.01)] and using [31, eq. (26)] the nth order moment of Z can be obtained in closed form as (see (18)).

3.3 Sequences of two sums of Nakagami-m variables

The following statistical metrics are related with the CH switching process investigated in the next section. Let us consider two independent sequences of RVs $Y_{1,j}$ and $Y_{2,j}$, with $j \in \mathbb{N}$, where for each j the PDF of $Y_{i,j}$ is described by (9). Furthermore, let us define a new sequence Z_n given as

$$Z_j = Y_{1,j} \quad \text{iff} \quad \begin{cases} Z_{j-1} = Y_{1,j-1} \text{ and } Y_{1,j} \geq \delta \\ \text{or} \\ Z_{j-1} = Y_{2,j-1} \text{ and } Y_{2,j} < \delta \end{cases} \tag{19}$$

where δ is a predefined threshold. It can be proved that by following the analysis provided in the appendix of [32], the CDF of Z_j has the following form

$$\mathcal{F}_{Z_j}(\gamma) = \begin{cases} \mathcal{C}\left[\mathcal{F}_{Y_{1,j}}(\gamma) + \mathcal{F}_{Y_{2,j}}(\gamma)\right], & \gamma \leq \delta \\ \mathcal{C}\left[\mathcal{F}_{Y_{1,j}}(\gamma) + \mathcal{F}_{Y_{2,j}}(\gamma) - 2\right] + \mathcal{D}, & \gamma > \delta \end{cases} \tag{20}$$

where

$$\mathcal{C} = \frac{\mathcal{F}_{Y_{1,j}}(\delta)\mathcal{F}_{Y_{2,j}}(\delta)}{\mathcal{F}_{Y_{1,j}}(\delta) + \mathcal{F}_{Y_{2,j}}(\delta)},$$

$$\mathcal{D} = \frac{\mathcal{F}_{Y_{1,j}}(\gamma)\mathcal{F}_{Y_{2,j}}(\delta) + \mathcal{F}_{Y_{1,j}}(\delta)\mathcal{F}_{Y_{2,j}}(\gamma)}{\mathcal{F}_{Y_{1,j}}(\delta) + \mathcal{F}_{Y_{2,j}}(\delta)}$$

Furthermore, in (20) $\mathcal{F}_{Y_{i,j}}(\cdot)$ is given by (10). The corresponding PDF of Z_j can be easily obtained as

$$f_{Z_j}(\gamma) = \begin{cases} \mathcal{C}\left[f_{Y_{1,j}}(\gamma) + f_{Y_{2,j}}(\gamma)\right], & \gamma \leq \delta \\ \mathcal{C}\left[f_{Y_{1,j}}(\gamma) + f_{Y_{2,j}}(\gamma)\right] + \mathcal{P}, & \gamma > \delta \end{cases} \tag{21}$$

where

$$\mathcal{P} = \frac{f_{Y_{1,j}}(\gamma)\mathcal{F}_{Y_{2,j}}(\delta) + \mathcal{F}_{Y_{1,j}}(\delta)f_{Y_{2,j}}(\gamma)}{\mathcal{F}_{Y_{1,j}}(\delta) + \mathcal{F}_{Y_{2,j}}(\delta)}$$

and $f_{Y_{i,j}}(\cdot)$ is given by (9).

3.3.1 Moments generating function: Substituting (21) in the definition of the MGF [25, eq. (5.62)] and using (9) and [21, eq. (6.643/3)] the MGF of Z_j, can be obtained as

$$\mathcal{M}_{Z_j}(s) = \mathcal{C}\sum_{i=1}^{2}\left[\mathcal{W}\left(\frac{\mathcal{A}_{\overline{\gamma}_i}}{s}, \alpha_i, \mathcal{B}_i\right) + \frac{1}{\mathcal{F}_{Y_{i,j}}(\delta)}\int_{\delta}^{\infty} f_{Y_{i,j}}(\gamma)\exp(-s\gamma)\,\mathrm{d}\gamma\right] \tag{22}$$

It is noted that in (22), the definite integral cannot be obtained in closed form and hence numerical evaluation methods will be employed, using any of the well-known mathematical software packages, for example, MATHEMATICA or MAPLE.

3.3.2 Moments: Substituting (21) in the definition of the moments, using (9), using [21, eq. (6.561/16)] and following a similar procedure to that used for deriving (10), the nth order moment of Z_j can be obtained in closed form as

$$\mu_{Z_j}(n) = \mathcal{C}\sum_{i=1}^{2}\left[\left(1 + \frac{1}{\mathcal{F}_{Y_{i,j}}(\delta)}\right)\mathcal{R}\left(\mathcal{A}_{\overline{\gamma}_i}, \alpha_i, \mathcal{B}_i\right) - \frac{\left(\delta\mathcal{A}_{\overline{\gamma}_i}\right)^{\{[(\Delta_{i^+})/2]+n\}}}{\mathcal{F}_{Y_{i,j}}(\delta)\mathcal{A}_{\overline{\gamma}_i}^{n}} \times \mathcal{G}_{1,3}^{2,1}\left(\mathcal{A}_{\overline{\gamma}_i}\delta \,\middle|\, \begin{matrix} 1 - \frac{\Delta_{i^+}}{2} - n \\ \frac{\Delta_{i^-}}{2},\ -\frac{\Delta_{i^-}}{2},\ -\frac{\Delta_{i^+}}{2} - n \end{matrix}\right)\right] \tag{23}$$

4 Mode of operation and received signal statistics

In this section, important statistical metrics of the received signal for both links in each side of the CH, namely the link between the AP and the CH (link 1) and the link between the CH and the nodes (link 2), will be studied, assuming 'shadowing' and 'correlated' effects are present. More specifically, the important situation where 'fully

$$\mu_Z(n) = \sum_{j=1}^{2}\mathcal{D}_j\mathcal{D}_\xi\mathcal{A}_{\overline{\gamma}_j}^{\left\{-\sum_{i=1}^{2}\{(\Delta_{i^+})/2\}-n\right\}}\mathcal{G}_{3,3}^{2,3}\left(\frac{\mathcal{A}_{\overline{\gamma}_\xi}}{\mathcal{A}_{\overline{\gamma}_j}}\,\middle|\, \begin{matrix} 1 - \frac{\Delta_{\xi^+}}{2},\ 1 - \alpha_j - \frac{\Delta_{\xi^+}}{2} - n,\ 1 - \mathcal{B}_j - \frac{\Delta_{\xi^+}}{2} - n \\ \frac{\Delta_{\xi^-}}{2},\ -\frac{\Delta_{\xi^-}}{2},\ -\frac{\Delta_{\xi^+}}{2} \end{matrix}\right) \tag{18}$$

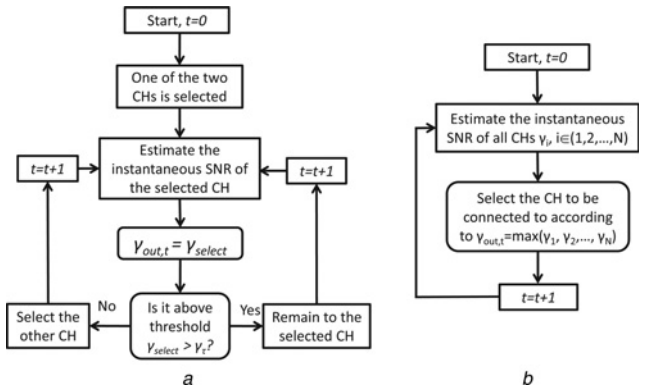

Fig. 3 *Mode of operation*
a CH switching algorithm
b CH selection algorithm

correlated shadowing' is present, will be investigated. This is the case where different paths simultaneously exhibit identical shadowing effects and have been studied many times in the past, for example [16, 17]. This type of shadowing is of great practical interest, since it arises in situations where the distance among the antennas is considerably smaller than the 'shadowing coherence distance' [33, 34].

Considering **link 1** and the downlink case the AP transmits a message to the CHs, employing the maximal ratio transmission (MRT) technique and assuming that perfect channel state information is available at the AP. For the uplink case, the CHs retransmit the decoded message, received from the nodes, to the AP, which combines the received signal replicas at each antenna by terms of MRC. Let $X_{\ell,i}$ represent the instantaneous SNR for the link between the ℓth antenna of the AP and the ith CH. Considering correlation among the links for the multipath effects, the total instantaneous SNR between the AP and the CH can be expressed as the sum of the individual SNRs $\gamma_i = \sum_{\ell=1}^{L_i} X_{\ell,i}$. In case that fully correlated shadowing effects are also presented, the analysis presented in Section 3.1 can be applied and the PDF of the output SNR, γ_i, is given by (9), the CDF by (10), the MGF by (12) and the moments by (13).

Considering **link 2** and assuming CH i is equipped with L_i antennas, the instantaneous SNR between the mobile nodes and each of the ith CH is $\gamma_i = \sum_{\ell=1}^{L_i} X_{\ell,i}$. Next, two strategies for selecting the CH to be connected are presented, namely (a) the CH selection algorithm (indicated as SE), and (b) the CH switching algorithm (indicated as SW). In Fig. 3, the mode of operation (in terms of a flowchart) for both these strategies is depicted.

4.1 CH selection

In CH selection strategy, CH providing the link with the highest instantaneous SNR is selected for the connection between the nodes and the AP. In this case the instantaneous SNR at the output of the nodes for the downlink (or at the output of the CHs for the uplink) is $\gamma_{se} = \max(\gamma_1, \gamma_2, \ldots, \gamma_N)$, see Fig. 3*b*. Considering the practically important case where the nodes may select and connect between 2 CHs, and based on the analysis presented in Section 3.2, the corresponding statistics of the output SNR, γ_{se}, are given as: the PDF by (15), the CDF by (14), the MGF by (17), and the moments by (18).

4.1.1 High SNR analysis: For high values of the average input SNR, that is $\bar{\gamma}_i \geq 30$ dB, simplified expressions for the MGF are evaluated. Starting from (17), using [30, eqs. (07.22.26.0001.01) and (07.22.06.0003.01)], yields the following closed-form approximated expression for $\mathcal{M}_{\gamma_{se}}(s)$

$$\mathcal{M}_{\gamma_{se}}(s) \simeq \sum_{j=1}^{2} \frac{\mathcal{D}_j \mathcal{D}_\xi \pi \csc(-\pi\Delta_{\xi^-})}{s^{[(\Delta_{j^+}-1)/2]}\sqrt{\mathcal{A}_{\bar{\gamma}_j}}} \exp\left(\frac{\mathcal{A}_{\bar{\gamma}_j}}{2s}\right) \times \left[\mathcal{H}_2\left(\alpha_\xi, \alpha_j, \mathcal{A}_{\bar{\gamma}_j}, \mathcal{B}_j, \mathcal{A}_{\bar{\gamma}_\xi}, \mathcal{B}_\xi, s\right) - \mathcal{H}_2\left(\mathcal{B}_\xi, \alpha_j, \mathcal{A}_{\bar{\gamma}_j}, \mathcal{B}_j, \mathcal{A}_{\bar{\gamma}_\xi}, \alpha_\xi, s\right)\right] \quad (24)$$

where

$$\mathcal{H}_2(x, y, z, q, w, r, s) = \frac{\Gamma(x+y) w^{[(x-r)/2]} \Gamma(x+q)}{\Gamma(x-r+1) x s^x} \times W_{[(1-y-q)/2]-x,\,[(y-q)/2]}\left(\frac{yz}{s}\right).$$

4.2 CH switching

For the CH switching strategy and in order to maintain a predefined QoS constraint the mobile nodes are able to switch between different CHs, according to the corresponding signal strength. More specifically, a CH is used for the communication link as long as the provided instantaneous SNR is above a predefined threshold; otherwise, the other CH within the same CH overlay is selected [35, eq. (62)], see Fig. 3*a*. In this way, unnecessary switchings can be avoided, compared with the CH SE mode. According to the protocol's mode of operation, the final instantaneous output SNR, γ_{sw}, will have the CDF given in (20), by substituting $Y_{i,j}$ with γ_i and representing the predefined QoS threshold δ as γ_τ. Hence, based on the analysis presented in Section 3.3, the corresponding PDF of γ_{sw} is given in (21), the CDF by (20), the MGF by (22) and the moments by (23).

4.2.1 High SNR analysis: Considering high values of the average input SNR, that is $\bar{\gamma}_i \geq 30$ dB, and starting from (22), representing the Bessel function as a generalised hypergeometric function, namely ${}_0F_1(\cdot;\cdot)$ [30, eq. (03.04.27.0005.01)], and by employing [30, eq. (07.17.06.0003.01)] a closed-form approximated expression can be obtained as

$$\mathcal{M}_{\gamma_{sw}}(s) \simeq \mathcal{C} \sum_{i=1}^{2} \left\{ \mathcal{W}\left(\frac{\mathcal{A}_{\bar{\gamma}_i}}{s}, \alpha_i, \mathcal{B}_i\right) + \frac{1}{\mathcal{F}_{\gamma_i}(\gamma_\tau)} \frac{1}{\Gamma(\alpha_i)\Gamma(\mathcal{B}_i)} \times \left[\Gamma(\Delta_{i^-})\left(\frac{\mathcal{A}_{\bar{\gamma}_i}}{s}\right)^{\mathcal{B}_i} \Gamma(\mathcal{B}_i, s\gamma_\tau) + \Gamma(-\Delta_{i^-})\left(\frac{\mathcal{A}_{\bar{\gamma}_i}}{s}\right)^{\alpha_i} \Gamma(\alpha_i, s\gamma_\tau)\right]\right\} \quad (25)$$

where $\Gamma(\cdot,\cdot)$ is the upper incomplete gamma function [21, eq. (8.350/2)].

5 Performance analysis

In this section, using the previously derived expressions for the instantaneous SNR of the links of both CH sides,

doi: 10.1049/iet-net.2012.0136

important performance quality indicators are studied. More specifically, the performance is studied using the OP and the BEP.

5.1 Outage probability

The OP is defined as the probability that the output SNR falls below a predetermined outage threshold γ_{th} and hence in our scenario an outage could occur if either one of the two links is in outage [36]. More specifically, for the communication link 1 and ith CH, the OP can be obtained as $P_{\text{out}_1} = \mathcal{F}_{\gamma_i}(\gamma_{\text{th}})$ using (10), whereas for link 2 it can be obtained as $P_{\text{out}_2} = \mathcal{F}_{\gamma_{\text{out}}}(\gamma_{\text{th}})$ using (14), for the CH selection algorithm, and (20), for the CH switching algorithm. Hence, the end-to-end (E2E) OP can be easily obtained as the complement event of having both links operating above a γ_{th}, that is, $P_{\text{out}_{\text{tot}}} = P_{\text{out}_1} + P_{\text{out}_2} - P_{\text{out}_1}P_{\text{out}_2}$. It is noted that for the CH switching case the optimal switching threshold γ_τ^* for minimum OP, can be obtained for $\gamma_\tau^* = \gamma_{\text{th}}$ [35].

5.2 Average BEP

In the DF strategy the CHs decode and retransmit the received signal to the destination (the AP or the nodes), thus resulting in an overall probability of error equal to [36]

$$P_{b_{\text{tot}}} = P_{b_1} + P_{b_2} - 2P_{b_1}P_{b_2} \tag{26}$$

where P_{b_1} denoted the average BEP obtained in link 1 and P_{b_2} is the average BEP obtained in link 2. In case of P_{b_1}, a direct evaluation of the BEP can be performed by averaging the conditional symbol error probability, $P_{\text{e}}(\gamma)$ [since $E_s = E_b \log_2 M$, $\overline{P}_{b_1} \simeq \overline{P}_{s_1}/\log_2 M$], over the PDF of γ_i, that is

$$\overline{P}_{s_1} = \int_0^\infty P_{\text{e}}(\gamma) f_{\gamma_i}(\gamma)\,\text{d}\gamma. \tag{27}$$

More specifically, for binary phase shift keying (BPSK) and square M-quadrature amplitude modulation, $P_{\text{e}}(\gamma) = A\text{erfc}(\sqrt{B\gamma})$, where erfc(·) denotes the complementary error function [21, eq. (8.250/1)] and A, B constants depending on the specific modulation scheme. Hence, substituting (9) in (27) and using [30, eq. (07.34.21.0011.01)] as well as [30, eq. (07.34.03.0890.01)] the SEP can be obtained in closed form as

$$\overline{P}_{s_1} = \frac{A\sqrt{\pi}\csc(-\pi\Delta_{i-})}{\Gamma(\alpha_i)\Gamma(\mathcal{B}_i)}\left[\mathcal{H}_3(\alpha_i, \mathcal{B}_i) - \mathcal{H}_3(\mathcal{B}_i, \alpha_i)\right] \tag{28}$$

where

$$\mathcal{H}_3(x, y) = \Gamma(x)\Gamma\left(x + \frac{1}{2}\right) \times \left(\frac{\mathcal{A}_{\bar{\gamma}_i}}{B}\right)^x {}_p\tilde{F}_q\left(x, x + \frac{1}{2}; x - y + 1, x + 1; \frac{\mathcal{A}_{\bar{\gamma}_i}}{B}\right)$$

For non-coherent binary frequency shift keying and differential BPSK (DBPSK), $P_{\text{e}}(\gamma) = A\exp(-B\gamma)$. Following a similar procedure as for deriving (12), $\overline{P}_{s_1}$ can be expressed in closed form as

$$\overline{P}_{s_1} = A\mathcal{W}\left(\frac{\mathcal{A}_{\bar{\gamma}_i}}{B}, \alpha_i, \mathcal{B}_i\right). \tag{29}$$

Furthermore, P_{b_2} can be easily obtained using the MGF expressions derived in the previous section, that is, (17) for the CH selection algorithm and (22) for the CH switching algorithm, and following the MGF-based approach [12]. Specifically, the BEP can be calculated: (i) directly for non-coherent DBPSK, that is, $P_{b_2} = 0.5\mathcal{M}_{\gamma_{\text{out}}}(1)$; and (ii) via numerical integration for Grey encoded M-PSK, that is, $P_{b_2} = \frac{1}{\pi \log_2 M}\int_0^{\pi - \pi/M} \mathcal{M}_{\gamma_{\text{out}}}\left[\frac{\log_2 M \sin^2(\pi/M)}{\sin^2\phi}\right]\text{d}\phi$. Moreover, for the CH switching algorithm, the optimum value of γ_T, that is γ_T^*, which minimises the BEP can be obtained by numerically solving $[\theta P_{b_2}(E)/\theta\gamma_T]|_{\gamma_T^* = \gamma_T} = 0$ [12, pp. 428].

6 Numerical results and discussion

In this section, selected numerical performance evaluation results are presented and discussed. These results include performance comparisons of several communication scenarios, employing various performance criteria and different fading and shadowing channel conditions. Firstly, E2E system performance results are presented, in terms of OP and BEP. Then, special attention is given to the CH-nodes communication link (link 2), where its performance is thoroughly investigated in order to understand the performance improvement of CH-selection algorithms in various communication scenarios in a better manner. The parameters considered in each communication scenario, can be found in Table 1. It should be noted that when small values for m (or α) are considered, strong multipath fading (or shadowing) effects are present and vice versa.

The rate of convergence of infinite series expressions in (17) has been investigated in Table 2. In this table, the minimum number of terms, N_{min}, for convergence of (17) in the range of $\pm 10^{-4}\%$ are provided, considering iid fading conditions [for the iid fading conditions $m_i = m$, $\alpha_i = \alpha$, $\rho_i = \rho$, $L_i = L$, $\gamma_i = \gamma$ for $i = 1, 2$], different values of m, α, $\bar{\gamma}$, ρ and $L = 2$. It is clear that only a few terms are needed in order to achieve target accuracy, whereas the required terms increase by increasing m, α and/or decreasing γ, ρ. Our research has also shown that similar rates of convergence were also obtained for different values of L.

Table 1 Parameter values for the communication scenario considered

Parameters	Values (scenario dependent)
APs antennas	$L_1 \in (2, 4)$
CHs antennas (for the AP link)	1
CHs antennas (for the nodes link)	$L_2 \in (2, 4)$
nodes antennas	1
correlation among APs antennas	$\rho \in (0, 1)$
correlation among CHs antennas	$\rho \in (0, 1)$
topology	randomly deployed APs, CHs and nodes
modulation scheme	DBPSK
fading parameter	$m \in (1, 4)$
shadowing parameter	$\alpha \in (0.5, 8)$

Table 2 N_{min} for convergence of (17) in the range of $\pm 10^{-4}\%$

$\bar{\gamma}$, dB	$\rho = 0.3$				$\rho = 0.7$			
	$m = 1$		$m = 3$		$m = 1$		$m = 3$	
	$\alpha = 1$	$\alpha = 3$	$\alpha = 1$	$\alpha = 3$	$\alpha = 1$	$\alpha = 3$	$\alpha = 1$	$\alpha = 3$
5	5	10	10	18	5	9	9	15
10	4	7	7	13	3	6	6	10
15	3	5	5	8	2	4	4	7
20	2	3	3	6	2	3	3	5

6.1 E2E performance results

In this subsection, iid fading and shadowing conditions have also been assumed. In Fig. 4, considering CHs with $L_2 = 2$ antennas (with $\rho = 0.2$) AP supporting different number of antennas L_1 (with $\rho = 0.2$) and DBPSK modulation scheme, the average BEP is plotted as a function of the average SNR per hop. Furthermore, the following fading conditions have been considered $m = 2$, $\alpha = 1.5$ for both links, whereas the investigation concerns (a) single CH communication, (b) CH with selection algorithm and (c) CH with switching. In this figure, it is clearly depicted that the worst performance is obtained in the single CH scenario, whereas the best is obtained when the CH selection algorithm is employed. It is also depicted that the performance also improves when the number of AP branches increases. In Fig. 5, considering the CH selection algorithm, the OP is plotted as a function of the normalised SNR per hop for different fading conditions and number of antennas employed in the APs and the CHs. More specifically, we have considered severe fading/shadowing conditions, that is $m = 1$, $\alpha = 1$, light fading/shadowing conditions $m = 3$, $\alpha = 3$. In this figure, it is illustrated that in all cases (for $L_1 = 4$, $L_2 = 2$ and for $L_1 = 2$, $L_2 = 4$) the best performance is obtained when light fading conditions are considered in link 1 and heavy fading conditions are considered in link 2. This is mainly because of the fact that the negative consequences

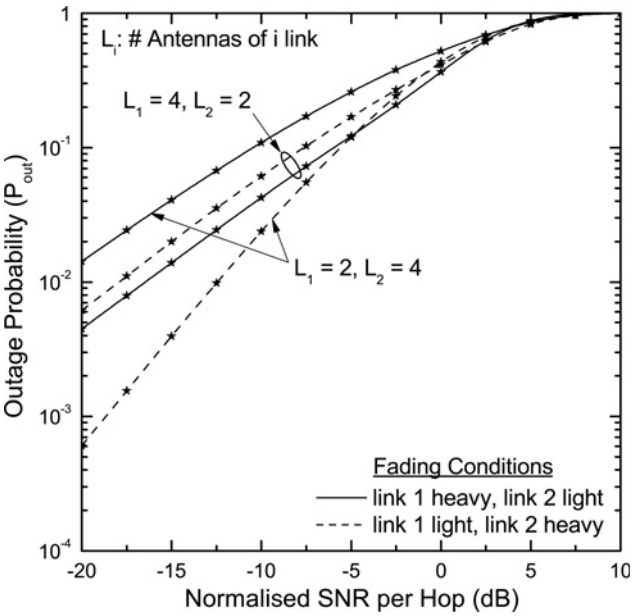

Fig. 5 *E2E OP against the normalised outage threshold per hop, $\gamma_{th}/\bar{\gamma}$, for various fading conditions*

of fading/shadowing have been effectively countermeasured using the proposed CH selection algorithm. It should be noted that similar performance result observations have also been reported in [37, 38]. More specifically, in both these works it was verified that the system performance, both in terms of BEP and OP, increases in case the number of receiver antennas employed also increases.

6.2 CH-nodes performance results

In Fig. 6, in order to investigate the energy efficiency that the CH selection algorithms induce to the nodes, normalised power consumption [the normalisation is defined by dividing the consumed power by the highest power

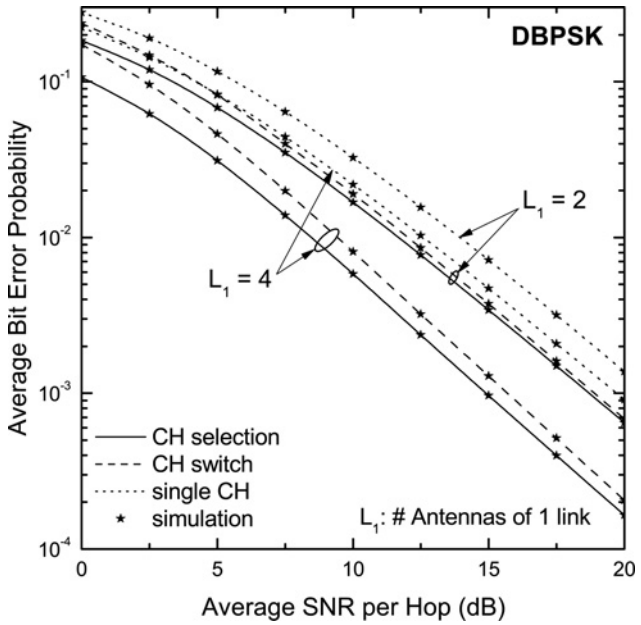

Fig. 4 *E2E average BEP against the SNR per hop for several values of L_1*

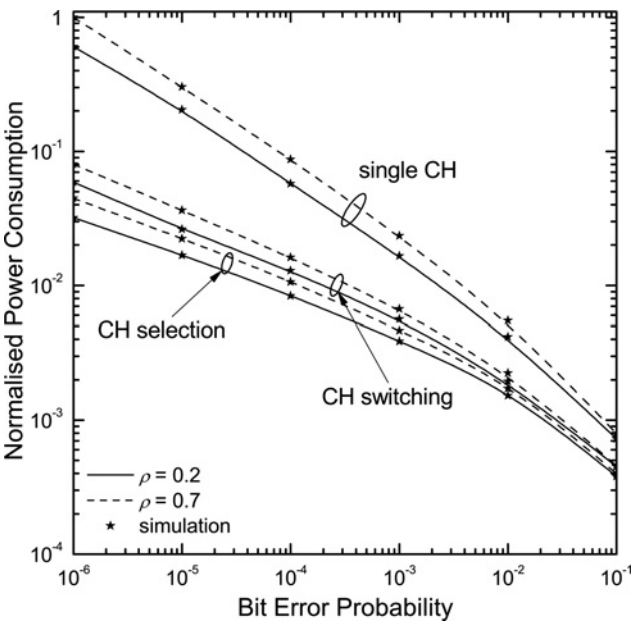

Fig. 6 *Node normalised power consumption as a function of the average BEP, for several values of the correlation coefficient*

doi: 10.1049/iet-net.2012.0136

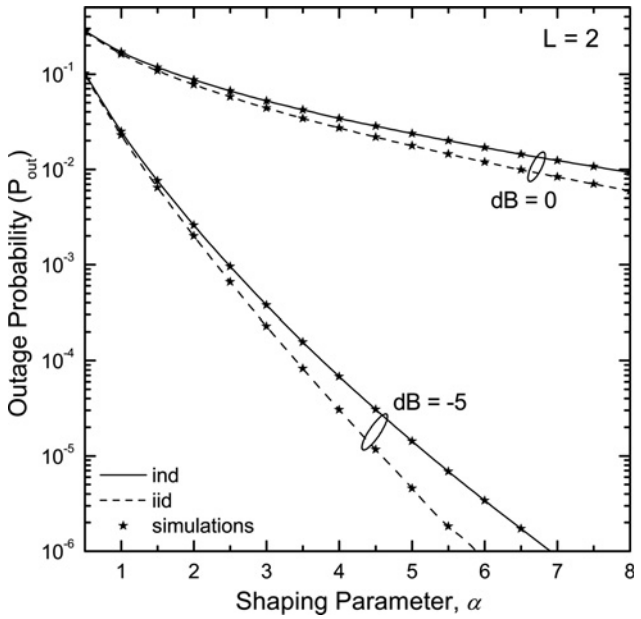

Fig. 7 *OP of CH selection algorithm as a function of the shadow shaping parameter α*

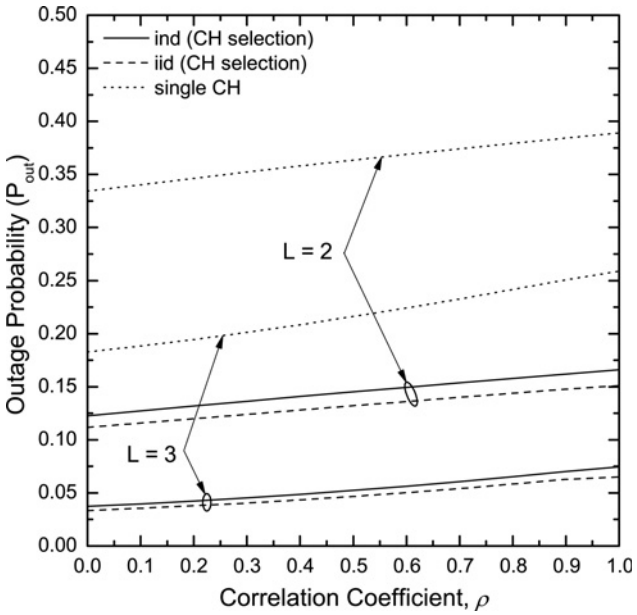

Fig. 8 *Node normalised power consumption as a function of the average BEP, for several values of the correlation coefficient*

consumed for obtaining BEP equal to 10^{-6}] is plotted as a function to the BEP of DBPSK. We have assumed $m = 2$, $L_2 = 2$, $\alpha = 2$ for all CH communication links, several values of ρ and optimum values for γ_τ for the case of switching algorithm. In this figure, it is shown that for the same QoS target, the lowest normalised power consumption performance is obtained when the CH selection algorithm is used, with, however, the switching algorithm having quite close performance. Another interesting observation in this figure is that power consumption also increases when the correlation coefficient of the multipath channel increases, since the diversity gain that is induced by the MAs reduces.

In Fig. 7, the OP of the CH selection algorithm is plotted as a function of α, for several values of the average input SNR and for iid and independent but non-identical distributed (ind) fading parameters. More specifically, for the ind case we have considered $m_1 = 1$, $\rho_1 = 0.7$ and $m_2 = 4$, $\rho_2 = 0.1$, for the iid case we have assumed for both CHs $m = (m_1 + m_2)/2$, $\rho = (\rho_1 + \rho_2)/2$, while in all cases $L = 2$ and $\alpha_i = \alpha$. It can be easily observed that the performance improves by increasing α, that is, the shadowing effects lessen, however, with decreasing rate of improvement. Another interesting observation is that the best performance is obtained when iid fading conditions are considered.

Finally, in Fig. 8, the OP of the CH selection algorithm is plotted as a function of ρ, considering ind and iid fading conditions, and several values of L. More specifically, for the ind case we have considered $a_1 = 1$, $m_1 = 1$, $a_2 = 3$, $m_2 = 4$, for the iid case we have $m = (m_1 + m_2)/2$, $\alpha = (\alpha_1 + \alpha_2)/2$, whereas for both cases $\rho_i = \rho$ and $L_i = L$. For comparison purposes the corresponding performance of single CH with MRC (or MRT) case is also illustrated. In this figure, it is depicted that the performance decreases as ρ increases, whereas the best performance is also obtained in case of iid fading. Furthermore, for both cases of selection algorithms, it is important to note the performance improvement when CH selection is employed, as compared with single CH reception. For comparison purposes, computer simulation performance results are also included in the figures, verifying the validity of the proposed theoretical approach.

7 Conclusions

In this paper, considering a composite fading environment (modelled by the exponential-correlated Nakagami-*m* fading and gamma distributed shadowing), a communication scenario where an AP is connected to the nodes through CHs, employing DF strategy, is studied. In this context, CH selection algorithms were proposed, where the nodes can switch between different CHs, according to the corresponding signal strength, in order to maintain a predefined QoS constraint. In addition, it was shown that when CHs are equipped with MA capabilities the negative consequences of multipath fading/shadowing are further degrading. Employing the proposed scheme, the reliability of CH-based networks significantly increases, whereas power consumption decreases. These improvements are more apparent in cases where connection to a CH may be not possible, because of multipath and/or shadowing effects, for example, in a mobile scenario. The theoretical results were validated via computer simulations. Our future research activities will include the scenario where a node may select a CH to connect to among L available as well as simpler diversity reception techniques.

8 Acknowledgments

This work has been performed under the framework of the ICE project ICE-5-258512 EXALTED, which is partly funded by the European Union. The authors would like to acknowledge the contributions of their colleagues. This information reflects the consortiums view, the Community is not liable for any use that may be made of any of the information contained therein. This work is also co-funded by the European Union and national resources under the National Strategic Reference Framework (NSRF) and the THALES research project: ENDECON.

9 References

1 Kortuem, G., Kawsar, F., Sundramoorthy, V., Fitton, D.: 'Smart objects as building blocks for the internet of things', *IEEE Internet Comput*., 2010, **14**, (1), pp. 44–51
2 Vermesan, O., Harrison, M., Vogt, H., Kalaboukas, K., Tomasella, M., *et al*.: (Eds.): 'The Internet of Things – Strategic Research Roadmap' 2009
3 Chatterjeo, M., Das, S.K., Turgut, D.: 'WCA: a weighted clustering algorithm for mobile ad-hoc networks', *Cluster Comput*., 2002, **5**, (2), pp. 193–204
4 Heinzelman, W., Chandrakasan, A., Balakrishnan, H.: 'An application-specific protocol architecture for wireless microsensor networks', *IEEE Trans Wirel. Commun*., 2002, **1**, (4), pp. 660–670
5 Dasgupta, K., Kalpakis, K., Namjoshi, P.: 'An efficient clustering-based heuristic for data gathering and aggregation in sensor networks'. IEEE Wireless Communications and Networking Conf. (WCNC), 2003
6 Sadek, A.K., Yu, W., Liu, K.J.R.: 'On the energy efficiency of cooperative communications in wireless sensor networks', *ACM Trans. Sensor Netw*., 2009, **6**, (1), pp. 5:1–5:21
7 Guo, M.H., Liaw, H.T., Deng, D.J., Chao, H.C.: 'Cluster-based secure communication mechanism in wireless ad hoc networks', *IET Inf. Secur*., 2010, **4**, (4), pp. 352–360
8 Shi, C., Zhao, H., Garcia-Palacios, E., Ma, D., Wei, J.: 'Distributed interference-aware relay selection for IEEE 802.11 based cooperative networks', *IET Netw*., 2012, **1**, (2), pp. 84–90
9 Younis O., Fahmy S., Santi P.: 'Robust communications for sensor networks in hostile environments', Intern., Works on QoS, 2004
10 Younis, O., Fahmy, S., Santi, P.: 'An architecture for robust sensor network communications', *Int. J. Distrib. Sensor Netw.*, 2005, **1**, (3), pp. 4305–327
11 Hashmi, S.U., Rahman, S.M.M., Mouftah, H.T., Georganas, N.D.: 'Reliability model for extending cluster lifetime using backup cluster heads in cluster-based wireless sensor networks'. IEEE Int. Conf. Wireless and Mobile Computing, Networking and Communications, 2010, pp. 479–485
12 Simon, M.K., Alouini, M.S.: 'Digital communication over fading channels' (Wiley, New York, 2005, 2nd edn.)
13 Cosşkun, A.F., Kucur, O.: 'Performance of maximal-ratio transmission with receive antenna selection in Nakagami-m fading channels'. IEEE 21st Int. Symp. Personal Indoor and Mobile Radio Communications (PIMRC), 2010, pp. 971–975
14 Renzo, M., Graziosi, F., Santucci, F.: 'A unified framework for performance analysis of CSI-assisted cooperative communications over fading channels', *IEEE Trans. Commun*., 2009, **57**, (9), pp. 2551–2557
15 Al-Ahmadi, S., Yanikomeroglu, H.: 'On the approximation of the generalized-K distribution by a gamma distribution for modeling composite fading channels', *IEEE Trans. Wirel. Commun*., 2010, **9**, (2), pp. 706–713
16 Zhu, C., Mietzner, J., Schober, R.: 'On the performance of non-coherent transmission schemes with equal-gain combining in generalized *K*-fading', *IEEE Trans. Wirel. Commun*., 2010, **9**, (4), pp. 1337–1349
17 Atapattu, S., Tellambura, C., Jiang, H.: 'Performance of an energy detector over channels with both multipath fading and shadowing', *IEEE Trans. Wirel. Commun*., 2010, **9**, (12), pp. 3662–3670
18 Bithas, P.S., Sagias, N.C., Mallik, R.K.: 'On the sum of Kappa stochastic variates and applications to equal-gain combining', *IEEE Trans. Commun*., 2011, **59**, (9), pp. 2434–2442
19 Bissias, N., Efthymoglou, G.P., Aalo, V.A.: 'Performance analysis of dual-hop relay systems with single relay selection in composite fading channels', *AEU – Int. J. Electron. Commun*., 2012, **66**, (1), pp. 39–44
20 Gagliardi, R.M.: 'Introduction to communications engineering' (Wiley, New York, 2005, 2nd edn.)
21 Gradshteyn, I.S., Ryzhik, I.M.: 'Table of integrals, series, and products' (Academic Press, New York, 2000, 6th edn.)
22 Abdi, A., Kaveh, M.: 'On the utility of the gamma PDF in modeling shadow fading (slow fading)', *IEEE Veh. Technol. Conf*., 1999, **3**, pp. 2308–2312
23 Abdi, A., Barger, H.A., Kaveh, M.: 'A simple alternative to the lognormal model of shadow fading in terrestrial and satellite channels'. IEEE Vehicular Technology Conf., Atlantic City, 2001, pp. 2058–2062
24 Bithas, P.S., Sagias, N.C., Mathiopoulos, P.T., Karagiannidis, G.K., Rontogiannis, A.A.: 'On the performance analysis of digital communications over generalized-*K* fading channels', *IEEE Commun. Lett*., 2006, **5**, (10), pp. 353–355
25 Papoulis, A.: 'Probability, random variables, and stochastic processes' (McGraw-Hill, New York, 1984, 2nd edn.)
26 Dong, C., Yang, L.L., Hanzo, L.: 'Multihop diversity for fading mitigation in multihop wireless networks'. 2011 IEEE, Vehicular Technology Conf. (VTC Fall), 2011
27 Wang, H., Ma, S., Ng, T.S.: 'On performance of cooperative communication systems with spatial random relays', *IEEE Trans. Commun*., 2011, **59**, (4), pp. 1190–1199
28 Yu, H., Stüber, G.L.: 'Outage probability for cooperative diversity with selective combining in cellular networks', *Wirel. Commun. Mobile Comput*., 2010, **10**, (12), pp. 1563–1575
29 Kotz, S., Adams, J.: 'Distribution of sum of identically distributed exponentially correlated gamma variables', *Ann. Math. Stat*., 1964, **35**, pp. 227–283
30 The Wolfram Functions Site. Available at: http://www.functions.wolfram.com, 2012
31 Adamchik, V.S., Marichev, O.I.: 'The algorithm for calculating integrals of hypergeometric type functions and its realization in REDUCE system'. Int. Conf. Symbolic and Algebraic Computation', Tokyo, 1990, pp. 212–224
32 Abu-Dayya, A.A., Beaulieu, N.C.: 'Analysis of switched diversity systems on generalized-fading channels', *IEEE Trans. Commun*., 1994, **42**, (11), pp. 2959–2964
33 Calabrese, F.D., Rosa, C., Anas, M., Michaelsen, P.H., Pedersen, K.I., Mogensen, P.E.: 'Adaptive transmission bandwidth based packet scheduling for LTE uplink'. IEEE 68th, Vehicular Technology Conf., 2008', VTC 2008-Fall', 2008
34 Rosa, C., Villa, D.L., Castellanos, C.U., *et al*.: 'Performance of fast AMC in E-UTRAN Uplink'. ICC'08, 2008 IEEE Int. Conf. Communications, 2008
35 Ko, Y.C., Alouini, M.S., Simon, M.K.: 'Analysis and optimization of switched diversity systems', *IEEE Trans. Veh. Technol*., 2000, **49**, (5), pp. 1813–1831
36 Hasna, M.O., Alouini, M.S.: 'End-to-end performance of transmission systems with relays over rayleigh-fading channels', *IEEE Trans. Wirel. Commun*., 2003, **2**, (6), pp. 1126–1131
37 Goel, S., Abawajy, l.H.: 'Performance of smart antennas with receive diversity in wireless sensor networks'. IEEE-lnt. Conf. Signal Processing, Communications and Networking, 2008
38 Goel, S., Abawajy, J.H., Kim, T.H.: 'Performance analysis of receive diversity in wireless sensor networks over GBSBE models', *Sensors*, 2010, **10**, (12), pp. 11021–11037

doi: 10.1049/iet-net.2012.0136